Magnetoresistance of Silver Bromide*

H. H. TIPPINS† AND FREDERICK C. BROWN
Department of Physics, University of Illinois, Urbana, Illinois
(Received 22 October 1962)

The magnetoresistance effect was investigated in high-purity zone-refined AgBr in order to obtain information about the conduction band structure in this material. The measurements were performed at 2°K and in magnetic fields up to 18 kG. The rate-of-drift method using a sensitive electrometer was employed to observe the transient photoconductivity both in the presence and absence of a magnetic field. Results of the experiments are consistent with the assumption of a spherically symmetric conduction band centered at $k=0$ as well as with an electron relaxation time of the form: $\tau=\tau_0(\epsilon/KT)^{3/2}$, with $\tau_0=1.1\times10^{-12}$ sec. During the course of the magnetoresistance measurements, a deviation from Ohm's law at high electric fields was noted. Some data on this "hot electron" effect are presented and briefly discussed.

I. INTRODUCTION

SPECULATIONS on the nature of the band structure in the silver halides have been of considerable interest for several years. By interpreting early experimental results on optical absorption and photoconductivity Seitz[1] suggested bands whose essential structure consisted of a simple conduction band centered at $k=0$, together with a more complicated valence band having a maximum not at $k=0$. Recently, measurements of photoconductivity and Hall mobility have been reported[2-5] on both AgBr and AgCl. These measurements have yielded considerable information on the nature of the electron-lattice interaction, particularly the scattering processes. However, magnetoresistance measurements are capable of providing important new information about the band structure and are now possible due to the availability of high-purity material.[6] It is the purpose of this paper to report the results of magnetoresistance measurements performed on photoelectrons at 2°K in zone-refined samples of silver bromide and to compare these results with theoretical equations developed for the case of an energy band of standard form, nondegenerate statistics, and very low carrier concentration. The theory appropriate to this situation is developed in the following section, and the pertinent experimental details are described in Sec. III. The results presented in Sec. IV are found to be in substantial agreement with this simple theory and offer good evidence that the conduction band is, in fact, of nearly standard form.

* Research supported in part by U. S. Air Force Office of Scientific Research. Based on a thesis submitted in partial fulfillment of requirements for the Ph.D. at University of Illinois.

† Present address: Aerospace Corporation, 2400 E. El Segundo Blvd., El Segundo, California.

[1] F. Seitz, Rev. Mod. Phys. **23**, 328 (1951).

[2] R. S. Van Heyningen and F. C. Brown, Phys. Rev. **111**, 462 (1958).

[3] F. C. Brown, J. Phys. Chem. Solids **4**, 206 (1958).

[4] K. Kobayashi and F. C. Brown, Phys. Rev. **113**, 507 (1959).

[5] D. C. Burnham, F. C. Brown, and R. S. Knox, Phys. Rev. **119**, 1560 (1960).

[6] F. Moser, D. C. Burnham, and H. H. Tippins, J. Appl. Phys. **32**, 48 (1961).

II. THEORY

The dark conductivity of the silver halides is less than $10^{-19}\ \Omega^{-1}\ \text{cm}^{-1}$ at liquid-helium temperatures. For typical low illumination intensities a photoconducting sample may have a conductivity of approximately $10^{-16}\ \Omega^{-1}\ \text{cm}^{-1}$. The illumination is normally kept to a minimum to reduce the buildup of internal polarization fields which make interpretation of experimental results very difficult. In materials of such low conductivity the Hall and magnetoresistance effects may be quite different from the corresponding effects occurring in a typical semiconductor or metal. In order to illustrate this statement we consider for simplicity materials containing only one type of carrier and compare the case of the normally insulating photoconductor with a typical semiconductor such as silicon or germanium. Consider first the case of a semiconductor. When a current flows in the semiconductor in the absence of a magnetic field, the electric field and current density vectors are parallel. This simple relationship is altered when a magnetic field is present. For example, if a magnetic field is applied in a direction perpendicular to the initial current direction, a transient flow of current will occur in the direction perpendicular to both the initial current direction and the applied magnetic field. This transient dies out very quickly, and the current flow returns to its initial direction. The steady-state condition is reached in less than 10^{-10} sec. During the period of transverse charge displacement a transverse electric field (the Hall field) is developed. The steady-state condition is such that the Hall field exactly cancels the Lorentz force of H on the average carrier. One may therefore consider that the net result of applying the magnetic field is to rotate the electric field out of its initial direction parallel to the current. Measurement of the transverse voltage that results gives the Hall constant, and the voltage drop in the current direction gives the resistivity in the presence of a magnetic field, i.e.,

$$\rho_{\text{exp}}=E_J/J=\mathbf{E}\cdot\mathbf{J}/J^2.$$

The change in ρ_{exp} produced by H is the quantity of interest in the magnetoresistance effect. We call

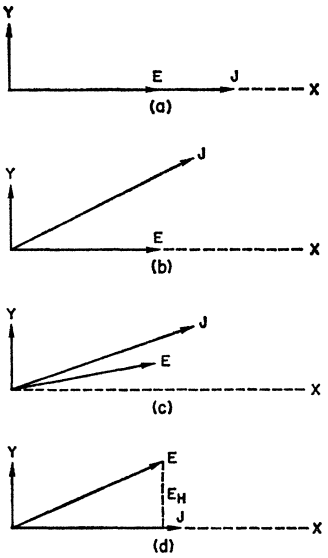

FIG. 1. Electric field and current density vectors during development of the Hall field in a semiconductor. (a) $\mathbf{H}=0$. (b) Instant after application of an $\mathbf{H}$ in z direction. (c) $t\cong$time required for E_H to develop. (d) $t\gg$time required for E_H to develop.

particular attention to the way the magnetoresistance measurement is performed, viz., a constant current $\mathbf{J}$ is passed through a sample and the electric field parallel to $\mathbf{J}$ is determined for both zero and finite H by measuring the voltage drop along $\mathbf{J}$. The vector diagrams of Fig. 1 illustrate the current and voltage relationships described above. Figure 1(a) is for a sample carrying a current due to an applied electric field $\mathbf{E}$ in the absence of a magnetic field. Immediately after application of a magnetic field H the situation shown in Fig. 1(b) obtains. A transverse current flows due to the Lorentz force of H on the carriers. In Fig. 1(c) the transverse Hall field has partially developed, and the transverse current decreased accordingly. In Fig. 1(d) the steady state has been reached, and the transverse current is now zero.

Many of the preceding remarks require modification for the insulating photoconductor. The time required for the establishment of internal fields is proportional to the resistivity of the material or equivalently to the reciprocal of the carrier concentration n, and can be several hours for n sufficiently small. In fact, due to the difficulty of interpreting the results when internal polarization fields are present, it is customary to go to the extreme and maintain the carrier concentration at as low a value as possible by using minimum illumination intensities. In this case the conductivity is measured by first establishing an electric field in the sample while it is in the dark. Then, the drift of charge which results when the sample is illuminated with light for a short time, is observed using a sensitive electrometer. This method can be employed both with and without a magnetic field. If the time during which such a measurement is performed is small compared to the time required to establish the transverse Hall field, then the applied electric field is the quantity that remains constant during the measurement; in particular, the transverse electric field remains at zero. Thus, for the insulating photoconductor, the net result of applying the magnetic field is to rotate the current density vector out of its initial direction parallel to the electric field. Here it is the component of $\mathbf{J}$ parallel to $\mathbf{E}$ that is measured and we can define

$$\sigma_{\text{exp}}=J_E/E=\mathbf{J}\cdot\mathbf{E}/E^2.$$

Particular attention should be paid to the difference in the definition of ρ_{exp} and σ_{exp}. In terms of the vector diagrams of Fig. 1 the situation in the insulating photoconductor remains as in Fig. 1(b) during the entire measurement time.

Within the range of electric fields such that Ohm's law is valid, the relation between current density and electric field may be written in the form:

$$J_i=\sum_j \sigma_{ij}E_j. \tag{1}$$

The quantities σ_{ij} in general form a second-rank tensor and, when a magnetic field is present, are functions of $\mathbf{H}$. The theoretical analysis of magnetoresistance is somewhat different for the two cases considered above. For the semiconductor $\mathbf{J}$ and $\mathbf{H}$ are specified, and Eqs. (1) solved for E_J; for the insulating photoconductor we specify $\mathbf{E}$ and $\mathbf{H}$, and solve Eqs. (1) for J_E. It should be remarked that although the quantity actually measured in this experiment is a conductivity, it will be convenient to refer to changes produced in $1/\sigma_{\text{exp}}$ by the applied magnetic field. This is done to conform with the more generally accepted practice of quoting values of the quantity $\Delta\rho/\rho$.

In an isotropic material the general form of the current density $\mathbf{J}$ in the presence of both an electric field $\mathbf{E}$ and magnetic field $\mathbf{H}$ is

$$\mathbf{J}=\sigma(H)\mathbf{E}+\alpha(H)\mathbf{E}\times\mathbf{H}+\gamma(H)(\mathbf{E}\cdot\mathbf{H})\mathbf{H}. \tag{2}$$

Within the framework of the classical theory, this equation is valid to all orders in H and for electric fields such that Ohm's law is valid. If we assume that a relaxation time τ can be defined, a solution of the Boltzmann transport equation yields expressions for the coefficients $\sigma(H)$, $\alpha(H)$, and $\gamma(H)$ in terms of integrals of the distribution function over wave-vector space. In addition we make the following assumptions:

(1) The conduction band consists of a single minimum centered at $k=0$. In a cubic crystal this means that to terms second order in k:

$$\epsilon=\hbar^2k^2/2m^*, \tag{3}$$

where ϵ is the energy, k is the wave vector, and m^* is the scalar effective mass of the carrier.

(2) The relaxation time τ is isotropic and can be written in the form:

$$\tau=\tau_0(\epsilon/KT)^p=\tau_0 x^p, \tag{4}$$

where K is Boltzmann's constant, T is the absolute temperature, and p is a constant characteristic of the particular scattering mechanism. Here we are assuming that a single scattering mechanism is operative. It should be noted that it is assumptions (1) and (2) that permit the theory appropriate to an isotropic material to be used as was tacitly assumed in writing down Eq. (2).

(3) Nondegenerate statistics are applicable with the equilibrium distribution function given by

$$f_0=\beta e^{-\epsilon/KT}=\beta e^{-x}, \tag{5}$$

where β is a parameter determined by the number of electrons per unit volume.

In this case the angular part of the scattering integrals can be carried out and the coefficients reduced to integrals over energy. The results are given as follows[7]:

$$\begin{aligned}
\sigma(H)&=\frac{4}{3}\frac{nm^*}{\pi^{1/2}}\left(\frac{e}{m^*}\right)^2\tau_0\int_0^\infty\frac{x^{p+3/2}e^{-x}dx}{1+\omega^2\tau_0^2x^{2p}},\\
\alpha(H)&=\frac{4}{3}\frac{nm^*}{\pi^{1/2}c}\left(\frac{e}{m^*}\right)^3\tau_0^2\int_0^\infty\frac{x^{2p+3/2}e^{-x}dx}{1+\omega^2\tau_0^2x^{2p}},\\
\gamma(H)&=\frac{4}{3}\frac{nm^*}{\pi^{1/2}c^2}\left(\frac{e}{m^*}\right)^4\tau_0^3\int_0^\infty\frac{x^{3p+3/2}e^{-x}dx}{1+\omega^2\tau_0^2x^{2p}},
\end{aligned} \tag{6}$$

where n is the carrier concentration, e is the magnitude of electronic charge, and $\omega=eH/m^*c$ is the cyclotron frequency ($c=10^8$ for "practical units"). Using the symbol "$\langle\ \rangle$"[8] to indicate an average of the form

$$\langle g\rangle=\frac{4}{3\sqrt{\pi}}\int_0^\infty gx^{3/2}e^{-x}dx, \tag{7}$$

the three coefficients become

$$\begin{aligned}
\sigma(H)&=\frac{ne^2}{m^*}\left\langle\frac{\tau}{1+\omega^2\tau^2}\right\rangle,\\
\alpha(H)&=\frac{ne^2}{m^*}\frac{\omega}{H}\left\langle\frac{\tau^2}{1+\omega^2\tau^2}\right\rangle,\\
\gamma(H)&=\frac{ne^2}{m^*}\frac{\omega^2}{H^2}\left\langle\frac{\tau^3}{1+\omega^2\tau^2}\right\rangle.
\end{aligned} \tag{8}$$

The following very useful relation follows immediately from the first and third equations above:

$$[\sigma(H)+\gamma(H)H^2]/\sigma(0)=1. \tag{9}$$

[7] Reference 5, Eqs. (20).

[8] F. J. Blatt, in *Solid State Physics*, edited by F. Seitz and D. Turnbull (Academic Press Inc., New York, 1956), Vol. 4, p. 240.

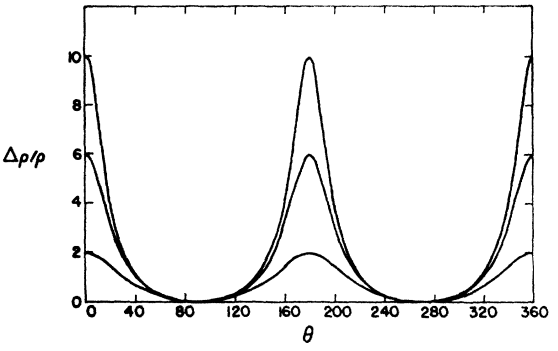

(a)

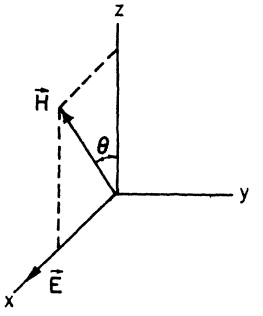

(b)

FIG. 2. Angular dependence of the magnetoresistance as given by Eq. (13). Each curve is for a different fixed H as $\mathbf{H}$ is rotated in a plane containing the electric field.

We now proceed to calculate the magnetoresistance for the transient case where the Hall field is zero. Take $\mathbf{E}=(E,0,0)$ and $\mathbf{H}=(H\sin\theta,0,H\cos\theta)$. Figure 2 shows the orientation of these vectors. We have from Eq. (2):

$$\begin{aligned}
J_E(H)&=J_x(H)=[\sigma(H)+\gamma(H)H^2\sin^2\theta]E,\\
J_E(0)&=\sigma(0)E.
\end{aligned} \tag{10}$$

The term in square brackets in Eq. (10) is the theoretical quantity to be identified with the σ_{exp} discussed previously. Using the definition:

$$M(\mathbf{H})=\frac{\Delta\rho}{\rho}=\frac{J_E(0)}{J_E(H)}-1$$

for the magnetoresistance, we obtain

$$M(\mathbf{H})=\frac{\sigma(0)}{\sigma(H)+\gamma(H)H^2\sin^2\theta}-1. \tag{11}$$

Two special cases of the relative field orientation are of particular interest.

(a) $\theta=0$, transverse case:

$$M_T=\frac{\sigma(0)}{\sigma(H)}-1=\langle\tau\rangle\Big/\left\langle\frac{\tau}{1+\omega^2\tau^2}\right\rangle-1. \tag{12}$$

(b) $\theta=90°$, longitudinal case:

$$M_L=\frac{\sigma(0)}{\sigma(H)+\gamma(H)H^2}-1.$$

TABLE I. Coefficients for weak- and strong-field magnetoresistance in a semiconductor with very low carrier concentration.

p	$M_{T0}/(\omega\tau_0)^2$	$M_{T\infty}/(\omega\tau_0)^2$	$M_{T0}/(\mu_H H/c)^2$	$M_{T\infty}/(\mu_H H/c)^2$	$M_{T0}/(\mu_M H/c)^2$	$M_{T\infty}/(\mu_M H/c)^2$
$-\frac{1}{2}$	1	0.5	1.275	0.637	1	0.5
0	1	1	1	1	1	1
$\frac{1}{2}$	3	2	1.087	0.724	1	0.667
$\frac{3}{2}$	120	6	1.577	0.0788	1	0.05

From Eq. (9) it follows that $M_L=0$. We, therefore, have the important result that for a spherical conduction band the longitudinal magnetoresistance is zero, a result which is also obtained for the steady-state case.

Equation (9) may also be used to eliminate $\gamma(H)H^2$ from Eq. (11), giving for the angular variation of M

$$M(\theta)=\frac{\cos^2\theta}{1+M_T\sin^2\theta}M_T. \tag{13}$$

It should be noted that $M(\theta)$ varies as $\cos^2\theta$ only for small M_T. Equation (13) is plotted as a function of θ for three different values of M_T in Fig. 2.

If we denote the transverse magnetoresistance in the limit of small H as M_{T0} and in the limit of large H as $M_{T\infty}$, we have from Eq. (12):

$$M_{T0}=\omega^2\langle\tau^3\rangle/\langle\tau\rangle, \tag{14}$$

$$M_{T\infty}=\omega^2\langle\tau\rangle/\langle 1/\tau\rangle. \tag{15}$$

Recalling the definition of ω, we, therefore, have the result that M_T is proportional to H^2 both at weak and at strong magnetic fields. This is in contrast to the result for the steady-state case which, although predicting an H^2 dependence at weak fields, predicts saturation (i.e., no H dependence) at strong fields. From Eqs. (4) and (7) we have

$$\langle\tau^n\rangle=(4\tau_0{}^n/3\sqrt{\pi})\Gamma(np+\tfrac{5}{2}). \tag{16}$$

Using Eq. (16), we obtain

$$M_{T0}=(\omega\tau_0)^2\Gamma(3p+\tfrac{5}{2})/\Gamma(p+\tfrac{5}{2}), \tag{17}$$

$$M_{T\infty}=(\omega\tau_0)^2\Gamma(p+\tfrac{5}{2})/\Gamma(-p+\tfrac{5}{2}). \tag{18}$$

It will also be convenient to express these limiting values of M in terms of the Hall mobility defined by

$$\mu_H=\frac{e}{m^*}\frac{\langle\tau^2\rangle}{\langle\tau\rangle}=\frac{e}{m^*}\tau_0\frac{\Gamma(2p+\frac{5}{2})}{\Gamma(p+\frac{5}{2})} \tag{19}$$

since this is a quantity directly measurable by other means. M_{T0} and $M_{T\infty}$ then become

$$M_{T0}=\left(\frac{\mu_H H}{c}\right)^2\frac{\Gamma(3p+\frac{5}{2})\Gamma(p+\frac{5}{2})}{[\Gamma(2p+\frac{5}{2})]^2}, \tag{20}$$

$$M_{T\infty}=\left(\frac{\mu_H H}{c}\right)^2\frac{[\Gamma(p+\frac{5}{2})]^3}{[\Gamma(2p+\frac{5}{2})]^2\Gamma(-p+\frac{5}{2})}. \tag{21}$$

Table I gives the values of the coefficients of $(\omega\tau_0)^2$ and $(\mu_H H/c)^2$ in Eqs. (17), (18), (20), and (21) for $p=-1/2$, 0, 1/2, 3/2. These are the respective values of p for scattering by acoustic modes, optical modes (or neutral impurities), dipole impurities, and charged impurities. Table I also gives the coefficients for expressing M_{T0} and $M_{T\infty}$ in terms of $(\mu_M H/c)^2$, where we define the magnetoresistance mobility by

$$\mu_M=(e/m^*)(\langle\tau^3\rangle/\langle\tau\rangle)^{1/2}. \tag{22}$$

This definition is suggested by the form of Eq. (14) which in terms of μ_M becomes

$$M_{T0}=(\mu_M H/c)^2. \tag{23}$$

This is simply a matter of defining the "mobility" in terms of a "relaxation time" which has particular physical significance for the problem at hand. We, then, obtain

$$M_{T\infty}=\left(\frac{\mu_M H}{c}\right)^2\frac{[\Gamma(p+\frac{5}{2})]^2}{\Gamma(-p+\frac{5}{2})\Gamma(3p+\frac{5}{2})}. \tag{24}$$

For intermediate values of H, we obtain from Eqs. (12) and (7)

$$M_T=\left(\int_0^\infty\tau x^{3/2}e^{-x}dx\Big/\int_0^\infty\frac{\tau x^{3/2}e^{-x}dx}{1+\omega^2\tau^2}\right)-1,$$

and from Eq. (4) this becomes

$$M_T=\Gamma(p+\tfrac{5}{2})\left[\int_0^\infty\frac{x^{p+3/2}e^{-x}dx}{1+\omega^2\tau_0{}^2x^{2p}}\right]^{-1}-1. \tag{25}$$

With the exception of $p=0$, the integrals in Eq. (25) cannot be expressed in closed form. They have, however, been evaluated numerically and the results are tabulated by Dingle *et al.*[9] In terms of the integrals tabulated in this reference, M_T becomes

$$p=-\tfrac{1}{2}:\quad M_T=\frac{1}{2\mathfrak{A}_2(\omega^2\tau_0{}^2)}-1, \tag{26}$$

$$p=0:\quad M_T=\omega^2\tau_0{}^2, \tag{27}$$

$$p=+\tfrac{1}{2}:\quad M_T=\frac{\omega^2\tau_0{}^2}{\mathfrak{A}_2(1/\omega^2\tau_0{}^2)}-1, \tag{28}$$

$$p=\tfrac{3}{2}:\quad M_T=\frac{1}{\mathfrak{S}_3(\omega^2\tau_0{}^2)}-1. \tag{29}$$

[9] R. B. Dingle, D. Arndt, and S. K. Roy, Appl. Phys. Sci. Res. **B6**, 144, 245 (1956).

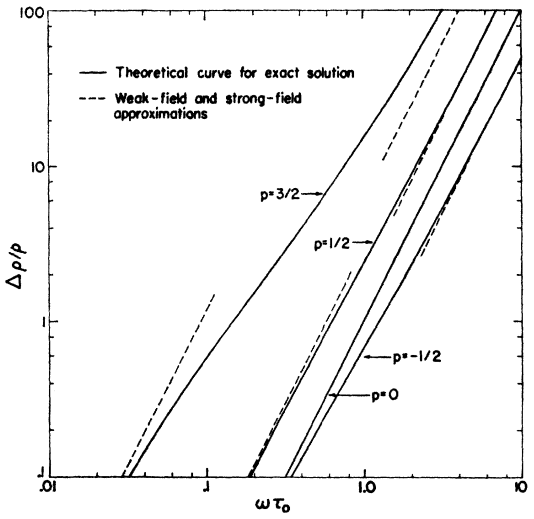

FIG. 3. Transverse magnetoresistance of an insulating photoconductor for the important scattering indices. The abscissa is proportional to H through $\omega=eH/m^*c$.

Theoretical curves of M_T versus $\omega\tau_0$, as calculated from the above formulas using reference 9, are shown in Fig. 3 for M_T between 0.01 and 100. In each case the curves approach the predicted weak- and strong-field asymptotes as given in Eqs. (17) and (18). It should be noted that the validity of the above solutions for large H is subject to speculation, since the classical approach is valid only for[10]

$$\omega\tau=(eH/m^*c)\tau\ll 1.$$

III. EXPERIMENTAL DETAILS

The study of electronic conduction processes in the silver halides is subject to a number of difficulties not encountered for typical narrow band gap semiconductors and metals.[3] The method of measurement which lends itself to the simplest interpretation is that of transient primary photoconductivity. This method was first employed by Lehfeldt[11] in measurements on insulating photoconductors in the early 1930's. A brief description of this method will now be given. For a more detailed description the reader is referred to the literature.[2] In discussing the experimental details, results, and conclusions we will continue to neglect the contribution of holes as was done previously in Sec. II. Although the experimental data on mobility and range of the hole at low temperatures in silver bromide are incomplete, this assumption appears to be a good one.[5]

Several alternative arrangements are possible for measuring the primary photoconductivity. The "rate-of-charge" method was selected because it offered certain experimental advantages. In order to understand this method, consider a crystal of thickness l placed between plane parallel "blocking" electrodes, one of which is connected to a battery and the other to a sensitive electrometer. The electrodes are blocked with thin insulating nonphotoconducting layers to prevent charge from entering or leaving the crystal. We assume that the crystal is at a sufficiently low temperature that ionic conductivity may be neglected. The dark conductivity of the crystal will then be very small ($<10^{-19}\ \Omega^{-1}$ cm^{-1}). If a potential difference is applied between the electrodes, an electric field is produced in the bulk of the crystal. The crystal will support such a field indefinitely if it is kept in the dark, and no charge displacement will be observed on the electrometer. If the crystal is now illuminated with light of appropriate wavelength, free electrons are released uniformly throughout the bulk of the crystal and the motion of these charges under the influence of the applied electric field is registered on the electrometer. A charge q, moving a distance x in the direction of the electric field, induces a charge qx/l on the electrode and makes a similar contribution to the total charge collected.

A free electron that is released by the light is eventually trapped by an imperfection within the crystal or is collected at the surface. After continued illumination, this trapped charge gives rise to an internal polarization field which can appreciably reduce the effect of the externally applied field and make accurate interpretation of future measurements impossible. It is, therefore, necessary to keep the intensity of illumination as low as is consistent with sensitivity requirements. Here we are dealing with a kind of a quasi steady-state situation whereby the trapping of the electrons is the process competing with the continuous excitation of free electrons by the incident light. Although the system is in a transient state, for times small compared to the time required to fill an appreciable fraction of the traps or the time required for the buildup of appreciable polarization field, the system may be treated as though it were in the steady state with constant values for carrier concentration and electric field. In this case we have

$$\dot{Q}=An_0e\mu E,$$

where $\dot{Q}$ is the rate at which charge is collected in C/sec, A the sample cross section in cm^2, n_0 the effective concentration of free electrons per cm^3, e the electronic charge in C, μ the mobility in cm^2/V sec, and E the electric field in V/cm.

On the basis of the preceding considerations, we are, therefore, assuming that a normally insulating photoconductor can be treated as a semiconductor with a free-charge density n_0 in thermal equilibrium with the lattice, where n_0 is determined by the incident light intensity and the trap density.[12] In this case the quantity $\dot{Q}$ that is measured experimentally is proportional to the

[10] A. H. Wilson, *The Theory of Metals* (Cambridge University Press, New York, 1954), p. 210.
[11] W. Lehfeldt, Nachr. Ges. Wiss. Göttingen **1**, 171 (1935).
[12] C. Kittel, *Introduction to Solid State Physics* (John Wiley and Sons, Inc., New York, 1956), 2nd ed., p. 516.

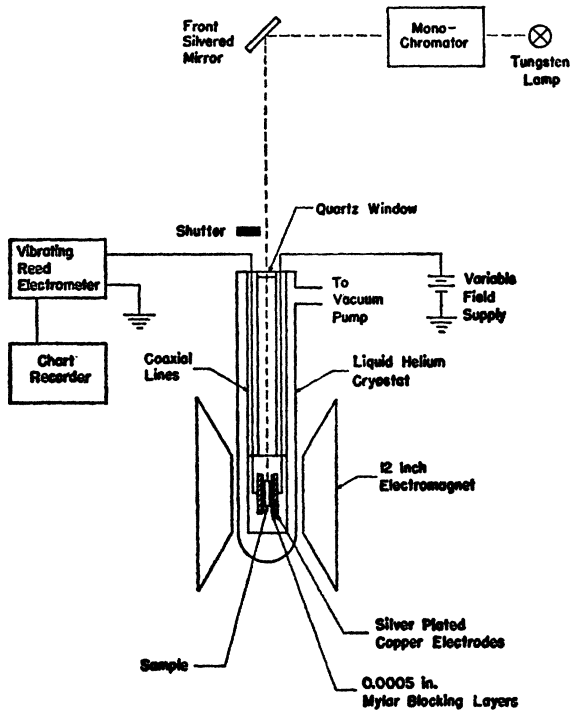

FIG. 4. Schematic diagram of apparatus. The entire sample chamber is immersed directly in pumped liquid helium.

theoretical quantity **J** discussed in Sec. II. The experimental magnetoresistance is then

$$\Delta\rho/\rho=[\dot{Q}(0)/\dot{Q}(\mathbf{H})]-1.$$

$\dot{Q}$ may conveniently be determined by connecting the electrometer output to a chart recorder and measuring the slope of the charge versus time response so obtained.

In order to obtain the high mobilities required to observe the magnetoresistance effect ($\mu_H \cong 10^4$ cm^2/V sec), it is necessary to work at liquid helium-temperatures to reduce the strong scattering due to the longitudinal optical modes. In addition, it is necessary to use samples of the highest available purity (zone-refined) to reduce the scattering due to charged impurities.

A schematic diagram of the apparatus used in this experiment is shown in Fig. 4. The electrometer employed was an Applied Physics Corporation Model 31 Vibrating Reed Electrometer. The electrometer was connected to a Varian Associates Model G-10 Chart Recorder. The light source consisted of the monochromator from a Beckman Model DU Quartz Spectrophotometer with a tungsten light source. Magnetic fields up to 18 kG were supplied by a Varian Model V-4012A Electromagnet System. The magnet was mounted on a calibrated turntable and could be rotated through the full 360° about a vertical axis. The magnetic field was measured with a rotating coil magnetometer. The Teflon sample holder was suspended from the top of the Dewar header by a length of thinwall cupro-nickel tubing and was surrounded by a brass can to shield the sample from external charges. The sample holder contained two silverplated copper electrodes, one fixed, and the other held against the sample by a light phosphor-bronze spring. Sheets of Mylar plastic 0.5 mil thick were placed between the electrodes and sample to act as blocking layers. The entire sample chamber was immersed directly in liquid helium which was maintained below the λ point by pumping. It was necessary to go below the λ point to reduce noise produced by the bubbling of the liquid helium. Since the Hall mobility is apparently independent of temperature below about 10°K,[5] one expects similar results at 2°K and at 4.2°K. The samples were cooled slowly from room temperature to liquid nitrogen temperature (about 20 h) to prevent strains which result from rapid cooling.

The wavelength of the illumination employed was 460 mμ. This wavelength is less than 1 mμ to the short-wavelength side of the steep rise in fundamental optical absorption in AgBr.[13] This choice of wavelength ensures a small absorption constant and, therefore, a uniform production of free electrons throughout the bulk of the material. The monochromator slit width was set at 0.01 mm for all measurements.

The following procedure was used in taking the measurements:

(1) With the electric and magnetic fields zero and the camera shutter that admits the light closed, the electrometer input is shorted.

(2) The electric field is switched on.

(3) The electrometer head is opened.

(4) The camera shutter is opened.

(5) After the electrometer has been integrating charge for about 25 sec, the magnetic field is switched on. For a typical field the small transient which occurs when the magnet is turned on lasts about 2 sec.

(6) The electrometer is allowed to integrate charge for another period of approximately 25 sec, then the shutter is closed.

(7) The electrometer head is shorted and the magnetic field is switched off.

For a typical measurement the shutter is open for approximately 60 sec and the total charge collected is about 10^{-13} C. It is possible to make approximately 60 such measurements before polarization effects are observed.

Preparation of Samples

Both samples used in the experiment were cut from ingot K-566-29-25 obtained from the Kodak Research Laboratories. This ingot is a section from the central portion of a larger AgBr ingot which was multiple zone-refined in a bromine atmosphere. A total of 81 zones were passed at a rate of $\frac{3}{5}$ in. per h. A spectro-

[13] F. C. Brown, T. Masumi, and H. H. Tippins, J. Phys. Chem. Solids **22**, 101 (1961).

chemical analysis of the ingot showed no detectable impurities except for possible traces of Fe (approximately 0.02 part/million). The ingot was cut with a tungsten carbide circular saw using xylene for a lubricant.

Sample KZR-2 is a rectangular parallelepiped obtained from the ingot by sectioning a slice approximately 2 mm thick. A microtome was used to remove about 0.15 mm of material from the two largest faces and one edge. (The sample was subsequently mounted in the holder so that the light entered the microtomed edge as indicated in Fig. 4.) After cutting and cleaning, the sample was etched in successively diluted HBr. The sample was then annealed on a carefully cleaned quartz plate in a continuously flowing helium atmosphere. The helium supply passed through a liquid-nitrogen trap before entering the furnace. The temperature cycle for the furnace was programmed to warm to 400°C in 20 h and then cool back to room temperature in 24 h. After annealing, the sample was polished on a flannel cloth wet with a 3% solution of KCN. All of the sample preparation operations described above were performed in subdued red light. The final dimensions of KZR-2 were 1.55 mm×5.2 mm×5.9 mm. Although this sample is not a single crystal, it has only one or two grain boundaries. The orientation of the single crystalline sections was not determined.

The sample designated KZR-110 is an oriented single-crystal disk 5.6 mm in diameter and 1.45 mm thick with the cylinder axis in the [110] crystallographic direction. The orientation was accomplished using x-ray back-reflection techniques. The cylindrical shape was produced by turning down the rough cut sample in a lathe with a tungsten carbide tipped tool. Approximately 0.15 mm was removed from each of the flat faces with the microtome. This sample was processed in exactly the same way as KZR-2 after the cutting operations.[14]

It was possible to estimate the unit range of electrons at 78°K for the Kodak ingot from a partial saturation curve obtained at this temperature on sample KZR-2. From these measurements the unit range was found to be approximately

$$w_0 = 2\times10^{-4}\ \text{cm}^2/\text{V}.$$

IV. EXPERIMENTAL RESULTS AND CONCLUSIONS

The magnetic field dependence of the transverse magnetoresistance for sample KZR-2 is shown in Fig. 5. The theoretical curve superimposed on the data points is the one obtained for charged-impurity scattering ($p=3/2$) and $\mu_H=5.86\times10^4$ cm²/V sec. In drawing a theoretical curve to fit the data we have only one parameter to be varied to make the fit (apart from the scattering index p). We may consider this single parameter to be τ_0, $\langle\tau\rangle$, μ_H, or μ_M since these quantities are all proportional to one another. Note that if the theoretical $\Delta\rho/\rho$ is plotted versus H on a log-log scale, the family of curves generated by varying the single parameter all have exactly the same shape; they are just displaced to the right or left relative to one another. If we set $m^*=0.3m$, we find that $\tau_0=1.1\times10^{-12}$ sec for the theoretical curve drawn on the data. The agreement between the theoretical curve and experimental points at low and intermediate fields is very good. The departure of the data from the theoretical curve for fields above about 5 kG is probably due to quantum effects and/or the relatively poor accuracy of the data for large $\Delta\rho/\rho$. For $\Delta\rho/\rho\sim1$ the data are accurate to about 5% while for $\Delta\rho/\rho\sim10$ the error may be as high as 15%. However, the departure may not be entirely due to experimental error since the trend away from the theoretical curve is fairly reproducible and was found in several different sets of data. It is not surprising that departures from the classical theory are observed at the highest fields for we have $\mu_H H/c\sim10$ in this region. Attempts to fit the data of Fig. 5 with theoretical curves for the other scattering mechanisms ($p=0$ and $\pm1/2$) were unsuccessful. This is good evidence that charged impurity scattering dominates at this temperature, in agreement with earlier observations.[5]

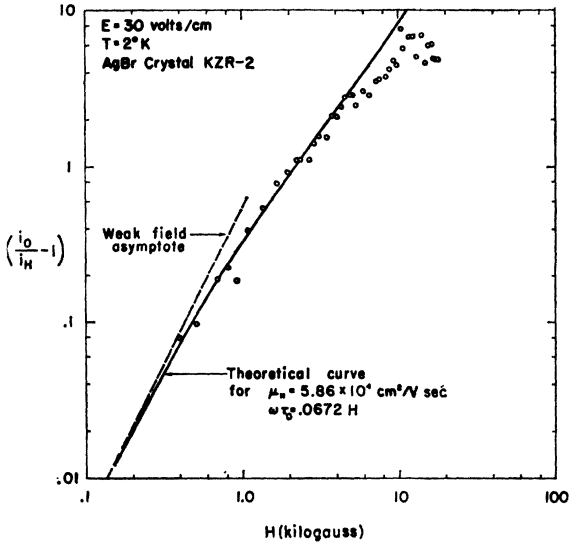

FIG. 5. Transverse magnetoresistance of zone-refined AgBr as a function of H. The solid line is a theoretical curve for $p=3/2$ computed from Eq. (29).

The data shown in Fig. 6 were also obtained for KZR-2. Here the magnitude of the magnetic field is held constant while the angle between **E** and **H** is varied through the full 360°. A magnet angle θ_M of 60° or 240° corresponds to **E** parallel to **H**, i.e., the longi-

[14] For measurements on KZR-110 the sample holder was constructed so that the electrode faces were perpendicular to the sample holder axis. The lower electrode was then the spring loaded one while the upper electrode consisted of a thin piece of quartz with a conducting NESA coating on the face adjacent to the sample. This permitted illumination of the sample through the electrode from the top as before.

tudinal effect, while a θ_M of 150° or 330° gives **E** perpendicular to **H**, i.e., the transverse effect. Figure 6 also shows the theoretical curve of this angular dependence calculated for the same μ_H used in calculating the theoretical curve of Fig. 5. Except for the difference in height of the two transverse peaks the agreement of the data with the theoretical curve is quite good. A point of particular interest is the vanishing of the longitudinal effect which is characteristic of a simple band structure. At $\theta_M=240°$ the longitudinal effect is only 0.015 and, even though a small effect is shown for $\theta_M=60°$, the ratio of the transverse to longitudinal effect exceeds 50:1. This may be compared to the results obtained for *n*-type germanium where the transverse effect is *smaller* than the longitudinal effect by approximately

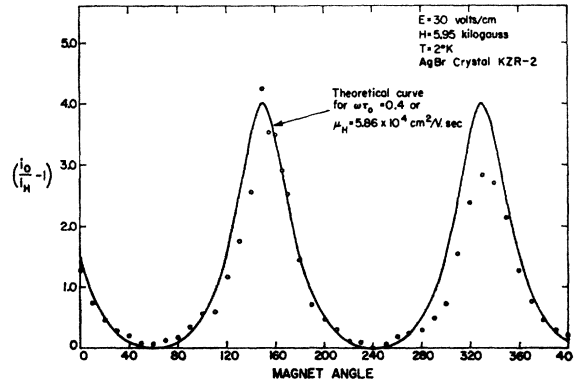

FIG. 6. Angular dependence of the magnetoresistance for fixed H in zone-refined AgBr. **E** lies in the plane of rotation of **H**. The solid line is the theoretical curve obtained from Eq. (13). Note that the same μ_H was used in calculating the theoretical curves of Figs. 5 and 6.

3:1.[15] The most reasonable explanation for the lack of symmetry of the transverse peaks is inhomogeneity of the sample. If the distribution of trapping centers throughout the sample is nonuniform, then the range of the electrons would vary with position in the sample. Suppose that a concentration gradient existed in the plane perpendicular to **E**. We would, therefore, expect $\dot{Q}(\mathbf{H})$ to differ from $\dot{Q}(-\mathbf{H})$ since, on the average, the carriers are swept in opposite directions, away from the drift direction, for **H** and $-\mathbf{H}$. At any rate the observed discrepancy is not serious and can be ignored entirely as far as conclusions about the band structure from these data are concerned.

Figure 7 shows a set of data taken on the oriented disk-shaped sample KZR-110. For these data the magnetic field is held constant in magnitude but rotated through the full 360° in the plane perpendicular to the electric field, which is in the [110] crystallographic direction. The dashed circle in Fig. 7 shows the average value of the experimental points. For a spherical conduction band and isotropic relaxation time, we should observe no variation in the magnetoresistance

[15] G. L. Pearson and H. Suhl, Phys. Rev. **83**, 768 (1951).

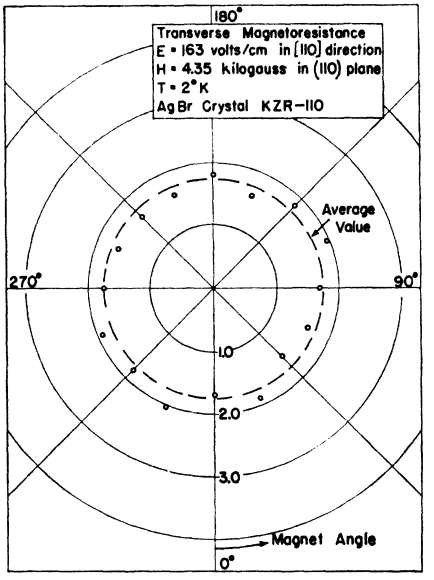

FIG. 7. Angular dependence of the transverse magnetoresistance for fixed H in zone-refined AgBr. **H** remains perpendicular to **E** while being rotated through the full 360°.

as the field is rotated. If the largest and smallest $\Delta\rho/\rho$ in the data of Fig. 7 are thrown out, the maximum departure from the mean is less than 10%. This departure is approximately the same as the estimated error and probably includes some contribution from sample inhomogeneity as discussed previously. In addition, the anisotropic relaxation time resulting from Coulomb scattering by charged impurities could also produce some anisotropy in such a plot of $\Delta\rho/\rho$. Several different sets of data were taken with these same experimental conditions. In each case an anisotropy similar to that present in Fig. 7 was observed.

Several attempts were made to observe the transverse magnetoresistance at 78°K. Even at a field of 18 kG the effect is just barely discernible and is of order 0.03. From the known Hall mobility[5] at this temperature, we expect an effect of order 0.01. The sensitivity of the rate-of-charge method to very small changes in σ is not

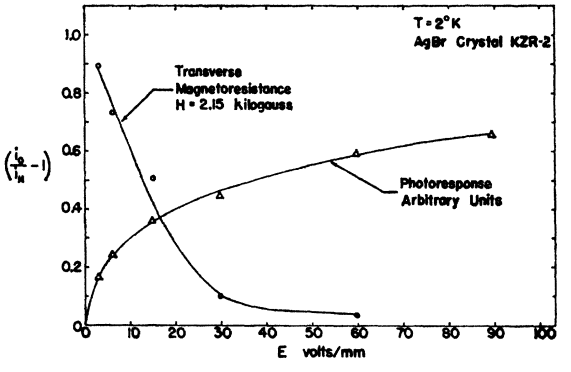

FIG. 8. Photoresponse and transverse magnetoresistance as a function of electric field in zone-refined AgBr.

sufficient to permit accurate magnetoresistance measurement in this temperature range.

During the course of the magnetoresistance measurements a nonlinear dependence of $\dot{Q}(0)$ on E was observed at the highest fields. Figure 8 shows the dependence of the photoresponse $\dot{Q}(0)$ and transverse magnetoresistance on electric field. Within the framework of the theory presented in Sec. II, $\dot{Q}(0)$ should be linear in E, and $\Delta\rho/\rho$ should be independent of E. We believe that the behavior illustrated in Fig. 8 arises from a breakdown of Ohm's law rather than saturation effects associated with the electron range. Although this sample has a relatively high unit range, the $\dot{Q}(0)$ versus E response showed only slight departures from linearity for $E=30$ V/mm at 78°K. At this temperature there is less trapping than at 2°K, and the longer unit range which results causes the $\dot{Q}(0)$ versus E curve to saturate at an even lower E than for 2°K.[2]

When an electron gains an amount of energy from the electric field between scattering events comparable to its thermal energy, a theory linear in E can no longer be expected to be valid. Under such conditions the conduction electrons are said to be "hot." Since these effects were beyond the scope of this experiment, their study was not pursued further. However, it may be stated that the general behavior of $\dot{Q}(0)$ for "large" fields is in accord with existing theories[16] (although this may be fortuitous). Also, the observed variation of $\Delta\rho/\rho$ with E is what one would qualitatively expect from the $\dot{Q}(0)$ versus E curve. We may interpret the hot electron effect in terms of a decrease of mobility with increasing electric field from the constant mobility normally observed when Ohm's law is valid. Thus, since $\Delta\rho/\rho\sim\mu^2$, one would also expect the magnetoresistance to decrease as E increases. A more complete study of $\dot{Q}(0)$ at high electric fields has subsequently been made by Masumi.[17] These insulating photoconductors are particularly well-suited to the study of hot electron effects because of the ease with which high electric fields can be obtained.

It should be noted that the magnetoresistance data shown in Figs. 5 and 6 were obtained for an electric field within the Ohm's law region. For the data of Fig. 7, it was necessary to use an electric field which somewhat exceeded the Ohm's law region. However, the electric field effects alone would not introduce any false anisotropy into these data.

The electric field effects also created some experimental difficulties. On the one hand, it was desirable to keep E within the Ohm's law region in studying the magnetoresistance effects so that the linear theory could be employed in interpreting the results. On the other hand, for high measurement sensitivity, it is desirable to use an E as large as possible so that illumination can be kept to a minimum. It was, therefore, necessary to compromise in selecting an electric field. Although the use of lower electric fields and higher illumination intensities (for a given sensitivity) does not appreciably speed up the onset of polarization, it was found that the rate of buildup of dark conductivity was approximately proportional to the light intensity. It is believed that the filling of very shallow traps is responsible for the observed buildup of dark conductivity. Thus, after continued illumination, the crystal becomes what amounts to an n-type semiconductor, having a number of electrons in shallow traps which are thermally excited to the conduction band. When such a condition is reached, performance and interpretation of the rate-of-charge measurements becomes very difficult. These considerations severely limited the data which could be taken on any particular run.

The data presented in Figs. 5 through 7 are in substantial agreement with the theory given in Sec. II, based on the model of a spherical conduction band centered at $k=0$, and are considered good evidence that such a model is correct for AgBr. Recent optical absorption measurements[13] have also been interpreted satisfactorily, using this conduction band model together with a more complicated valence band structure similar to the model originally proposed by Seitz. Still more recently, cyclotron resonance has been obtained in AgBr at 70 kMc/sec and shows no appreciable change as the magnetic field is rotated with respect to the crystal axes.[18]

ACKNOWLEDGMENTS

The authors would like to acknowledge helpful discussions with Professor J. Bardeen, Dr. R. Swank, and F. E. L. Witt during this investigation. The section of zone-refined AgBr ingot furnished by Dr. F. Urbach of the Kodak Research Laboratories is sincerely appreciated. One of the authors (H. H. T.) received the aid of a fellowship provided by the General Electric Company.

[16] W. Shockley, Bell System Tech. J. **30**, 991 (1951).
[17] T. Masumi, Phys. Rev. **129**, 2564 (1963).
[18] G. Ascarelli and F. C. Brown, Phys. Rev. Letters **9**, 209 (1962).